Investigation of injury mechanisms in sledging accidents involving children and adults

Stefan Smit, Johanna Trauner-Karner, Michael Nader, Desiree Kofler,
Nico Erlinger, Florian Feist, Corina Klug

Abstract   In this study, injury mechanisms in sledging accidents, which is often regarded as a harmless activity, are investigated. It aims to provide recommendations regarding helmet use and the correct seating position of children when riding together with an adult. Two Human Body Models, the PIPER 6YO (v0.99) and the THUMS-AM50O (v4.02), were used to simulate child and adult sledge riders colliding with a tree. This setup was chosen as collisions with stationary objects frequently lead to serious or even fatal injuries according to the accident analysis. Simulations of a child riding alone with and without helmet as well as simulations of a child and an adult riding together were performed. Different impact velocities (5–30km/h) and impact angles (0–45°) were simulated. Kinematic and strain-based head injury criteria were evaluated alongside strains in cortical bones of the thorax, upper and lower extremities.

Helmet-wearing reduced head injury criteria, regardless of impact velocity and impact angle, although the effect was not equally pronounced for all criteria. When riding together with an adult, children should sit in the rear since this reduces injury metrics for the head and lower extremities. The simulations highlight the benefit of wearing a helmet when riding a sledge.

Keywords   Sledging, sports injury, helmet, PIPER child model, THUMS

I. INTRODUCTION

Sledging is a popular recreational sport in alpine countries, such as Austria. Literature focusing on sledging injuries usually uses retrospective data from trauma centres or personal interviews to obtain data on injured body regions and injury mechanisms. Frequently observed scenarios include collisions with stationary objects [1]–[9], falls [1], [4]–[5], [7], and collisions with people within the sledging area, e.g. people walking back up the slope for another run [1], [3], [10]. When focusing on sledging accidents involving major trauma, collisions with stationary, almost rigid objects, such as trees or lift poles, are the predominant accident type [4], [11].

Although some studies claim that one can achieve '*considerable*' or '*high*' speeds when riding a sledge, the velocity of people while sledging was measured in only one study, using a radar gun. The mean velocity was about 30 km/h, while the maximum velocity recorded was approximately 40 km/h [12].

Frequently injured body regions are the head [1], [4]–[5], [9], [13]–[14], neck [3], [5], [13], upper extremities [7], [14]–[15] and lower extremities [1], [4], [7], [14], [16]. Additionally, injuries to the thorax [6], [15], pelvis [15], spine [3], [6], [8], [15] and internal organs [3], [14] were observed in previous studies. Although injury frequencies differ among those publications, injuries to the same body regions were recorded. In fatal sledging accidents, head injuries are the most frequent cause of death [11]. Similar injury patterns were found for children and adults.

The share of people wearing a helmet when sledging was found to be only between zero [2], [9], [12] and 7% [7]. The injury risk associated with sledging accidents is often underestimated. It is often assumed that children are not riding fast enough to sustain serious injuries.

In this study, finite element (FE) human body models (HBMs) are applied to investigate injury mechanisms and injury metrics of sledge riders colliding with an almost rigid obstacle. The premise of this study was to derive recommendations regarding helmet use and the proper seating position for children riding together with adults. The aim was to analyse the helmet effectivity for different impact scenarios at varying impact velocities and

angles. Furthermore, the amount of additional load for the most common seating configuration (child sitting in front of the adult) was investigated and compared to an alternative configuration, where the child is sitting behind the adult.

II. METHODS

Accident analysis

In order to obtain injury patterns in sledging accidents, sledging accidents from the year 2019, recorded in the Injury Database Austria (IDB) were analysed. The IDB Austria is maintained by the Austrian Road Safety Board (KFV) Data from various accident types, including accidents resulting from sports, traffic or from activities related to leisure, household, work and school are collected in the IDB.

About 15,000 face-to-face interviews are conducted annually with accident victims in eleven Austrian hospitals (both in- and out-patients). A standardised questionnaire is used to gather detailed accident information. Data includes products involved (e.g. sports equipment, vehicles, tools, furniture, etc.), accident causes as well as injuries and their severities. Precise descriptions of these accidents provide valuable insights into the mechanisms and circumstances leading to injuries. Hospital discharge statistics are used to extrapolate the IDB sample for the entire federal territory of Austria.

Numerical model

A simplified model of a wooden sledge was created. The geometry was modelled based on measurements from an existing standard sledge. The frame was modelled of solid elements, the seat of shell elements. The entire sledge model is rigid (frame and seat), as it is not expected that the sledge will break in the collision. The sledge model consists of approximately 17,700 elements and has a mass of about 4.5 kg. A tree with a diameter of 50 cm, representing an approximately 50-year-old spruce [17], was chosen as the rigid object. Assuming the tree does not deform due to the impact of the sledge or the riders, the inner part tree consists of rigid shells, while an outer layer of 3 cm thickness was modelled using solid elements to achieve a realistic stiffness for the impacts. Material properties, which are used to simulate road restraint systems (wooden guardrails), were assigned to the outer solid layer of the tree [18]–[19].

The PIPER-6YO (v0.99) and the THUMS-AM50-O (v4.02) were used to represent a child and an adult person in a sledge ride, respectively. These were positioned in a typical sledging position using pre-simulations. For the PIPER model two different positions, representing a child sitting at the front (Fig. 1) and in the back (Fig. 2), were derived with different arm positions. For the THUMS, one position was sufficient for the front and back seat.

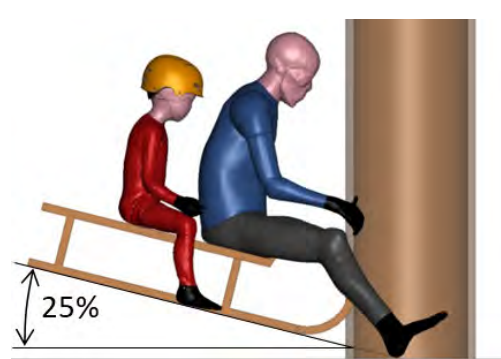Fig. 1. Frontal impact, child sitting in front of the adult person.

Fig. 2. Frontal impact, child sitting behind the adult person.

A hard shell helmet, developed and validated in previous studies [20]–[21], was used for the child. The helmet validation was done based on test data obtained from bicycle helmet tests according to EN 1078 [22] and additional tests at an impact velocity of 6.5 m/s, an impact angle of 30° as well as normal and increased friction between helmet and anvil [20]. The innermost low-density foam layer of the helmet was not modelled since it does not absorb any energy in case of impact. The helmet was positioned such that the gap between head and helmet was equal at the front, back and top, and the eyebrow-to-helmet-leading-edge distance was 20 mm ('two-finger-rule', Fig. 3) [20]. The chinstrap of the helmet model is represented by 1D elements ('MAT_SEATBELT'). The chinstrap was attached to the head using two sliprings rigidly attached to the jawbone of the PIPER. The

circumferential strap was adjusted to represent a proper helmet fit (no slack).

To simulate a realistic sledge ride, a slope of 25% (approx. 14°, Fig. 1, Fig. 2) was implemented, representing the maximum incline of an *'easy'* skiing slope (blue marking) [23]. The initial velocity and the lateral offset between the centrelines of the sledge and the tree were defined for each simulation (Fig. 4). By moving the sledge to the side (lateral offset in Fig. 4) the theoretical impact plane and theoretical head impact point were obtained. Both the impact plane and the impact point are theoretical, since the head may impact the tree at a different location due to the kinematics prior to the head impact, influenced by the interaction between sledge and tree and sledge and occupant, respectively.

Simulations were performed using the LS-DYNA MPP R9.2.0 single-precision solver running on a HPC Linux cluster (64 CPUs). The effective simulation time step of the THUMS (0.3996 µs) was used in all simulations, since this was smaller than the one of the PIPER model (0.432 µs) and PIPER is supposed to run stable using a smaller time step.
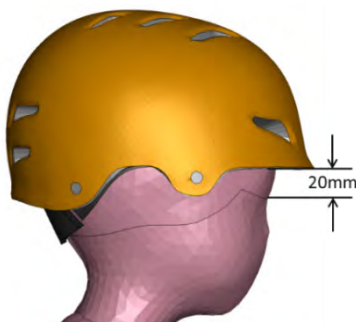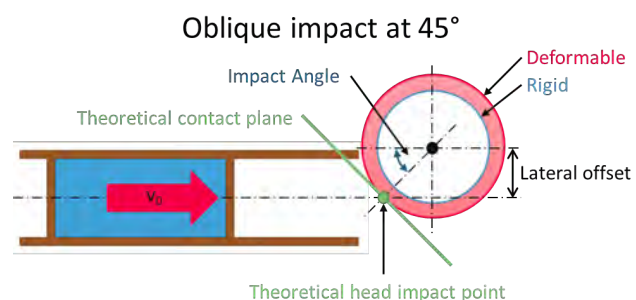

Fig. 3. Helmet position PIPER.

Fig. 4. Schematic definition of the impact configuration.

Simulation matrix

Twenty-five simulations, representing two main setups, were performed. The full simulation matrix, including varied parameters and their values for each individual simulation, is provided in the Appendix (TABLE A1).

The first setup aimed to identify the protective effect of wearing a helmet. Therefore, simulations of a child riding alone with and without helmet were performed. Impact velocities were varied from 5 km/h to 30 km/h in 5 km/h steps. At an impact velocity of 20 km/h, four different angles (0°, 15° 30° and 45°) were simulated to explore differences between frontal and oblique impacts. For the child with helmet, simulations at higher impact velocities (25 km/h and 30 km/h) were performed to explore potential performance limits of the helmet.

The second main configuration was used to derive recommendations regarding the proper seating position for the child, when riding together with an adult. Therefore, back-to-back simulations with the child sitting at the front (Fig. 1) and at the rear (Fig. 2) were performed. Different impact angles (0°, 15° and 30°) were simulated at an impact velocity of 20 km/h. Additionally, simulations at 25 km/h and 30 km/h were performed at an impact angle of 30°. In those simulations the child was always wearing a helmet. The adult was not wearing a helmet in any of the simulations.

Evaluation

Different criteria were evaluated, analysing different body regions. For the head, the kinematic-based criteria HIC [24] and DAMAGE [25] as well as maximum principal strains (MPS) of the brain and the skull were evaluated.

While HIC uses linear head accelerations, DAMAGE (Diffuse Axonal Multi-Axis General Evaluation) is based on rotational head accelerations. When calculating DAMAGE, the maximum angular accelerations are normalized by directionally dependent thresholds. DAMAGE aims to predict maximum brain strains. Currently used thresholds for DAMAGE correspond to a 50th percentile adult human brain model [25].

To evaluate the time-histories of PIPER, a history node (*DATABASE_HISTORY_NODE) was created at the geometric centre of the skull. Its motion was interpolated from all nodes of the cortical skull, using a *CONSTRAINED_INTERPOLATION keyword. Acceleration signals were written at 10 kHz (timestep: 0.1 ms) and filtered (CFC1000), as suggested in SAE J211 [26], before evaluating HIC and DAMAGE. To be able to evaluate DAMAGE, head accelerations were written with respect to a local coordinate system according to SAE J211 [26]. The same approach was used for the THUMS model.

Brain strains (95th MPS) were evaluated for solid elements of the brain. The brain of the PIPER consists of

17,011 elements (V = 1.359 l; m = 1.409 kg). Hence, the characteristic length of the brain elements is approx. 4.3mm when assuming perfect cubic elements. In comparison, the brain of the THUMS (cerebrum, cerebellum, brainstem) consist of 118,840 solid elements (brain volume: 1.453 l; m = 1.453 kg) Hence, the characteristic element size is about 2.3mm. Element data were written to a binout-file at 1 kHz (element data; timestep: 1 ms). The evaluation procedure was the same for PIPER and THUMS.

The 99th MPS of the skull was evaluated analogously to brain strains using strain data from the cortical skull bone of the respective HBMs. Additionally, the strains in cortical bones of the thorax (ribs, clavicle), upper extremities (humerus, radius, ulna) and lower extremities (femur, tibia, fibula) were evaluated. Since the bones of the lower arm (radius, ulna) are not deformable (*MAT_RIGID) in PIPER, those bones could not be considered in strain evaluation for PIPER. Detailed information on parts considered in strain evaluation for PIPER can be found in the Appendix (TABLE A2). For the THUMS, the stains were evaluated for the same bones as for PIPER.

All injury metrics used in this study were used for qualitative comparisons only. No injury risk assessment was performed since the sledge and tree model were not validated.

Simulation data were post-processed using the open-source post-processing tool Dynasaur [27], capable of reading and processing data from LS-DYNA binout files, based on user-defined calculation procedures. Exemplary calculation procedures for evaluating DAMAGE and 95th MPS in the brain can be found in the Appendix.

III. RESULTS

Accident analysis

In 2019, a total of 63 personal interviews with victims of sledging accidents were recorded in the IDB. When extrapolated to the Austrian population (using hospital discharge statistics), this resulted in annual number of approximately 2,200 injuries from sledging accidents, including two fatal accidents. About half (49%) of the injuries were sustained by adults, while children (35%), adolescents (12%) and seniors (4%) accounted for the remaining proportions of the injured population. While around 40% of the injured persons were female, about 60% were male. The three most frequent injury types were bone fractures (61%), followed by injuries to tendons and muscles (20%) and contusions (12%).

The three main scenarios were falls (67%), collisions (28%) and other accidents (5%), including bruises or being jammed. The most frequent accident causes were misjudgement and lack of skill (48%), overconfident riding (20%) and unexpected slope conditions (e.g. ice or bumps, 12%).

Simulation results of Child riding alone

In frontal impacts, the sledge impacted the tree, instantly decelerating and going into a slight rebound. The child slides forward on the seat, until contact between the thighs and the frontal structure of the sledge occurred, loading the femur of the child. This caused the feet to lift from the ground and the child's thorax and head to tilt forward, so that the head contacted the tree (Fig. A). After this impact, the head rebounded from the tree, causing increased strains in the ribs (Fig. A7). Only in the case of an impact velocity of 5 km/h did no pronounced head rebound occurred. For simulations without helmet, slight contact between thorax and tree was observed at 20 km/h.

For oblique impacts, especially at higher impact angles (30°, 45°), different kinematics were observed. After the sledge contacted the tree, rotational motion was initiated. This caused the child and the sledge to rotate, resulting in asymmetric loading of the child's thighs. Additionally, a more pronounced forward rotation of the head and the thorax occurred before the head contacted the tree. Due to the modified head impact point, there was no pronounced head rebound and therefore less neck extension than in frontal impacts occurred. In case of the 45-degree impact, the child was thrown off the sledge and the thorax did not hit the tree.

The kinematic sequence was found to be similar for simulations with and without helmet. The only difference in the kinematics was a slightly dampened head rebound when wearing a helmet.

HIC ranged from 166 to 8,415 without helmet, and from 23 to 7,807 with helmet (Fig. 5, Fig. 6), increasing with higher speeds and decreasing with increasing impact angles (oblique impacts). For frontal impacts with helmet the HIC shows exponential growth with increasing impact velocities (hatched bars in Fig. 5). Fig. 6 shows HIC values at 20 km/h for different impact angles. On average, HIC decreases by 85.2% in frontal impacts, by 86.1% in oblique impacts and by 85.6% overall, when wearing a helmet. Criteria values for all simulations can be found in the Appendix (TABLE A3).
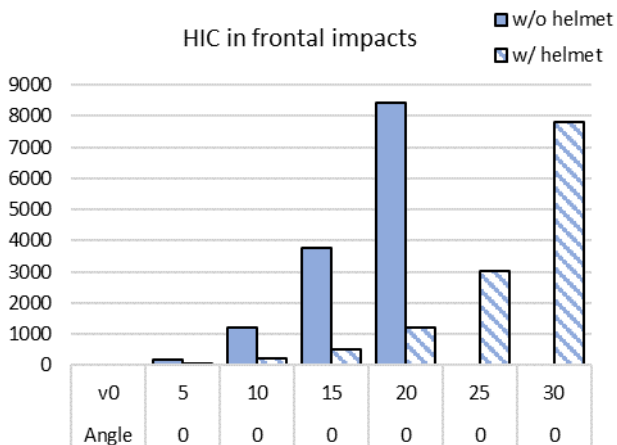
Fig. 5. HIC with and without helmet in frontal impacts (0deg) for different impact velocities; no simulations without helmet were conducted for $v_0 > 20$ km/h.
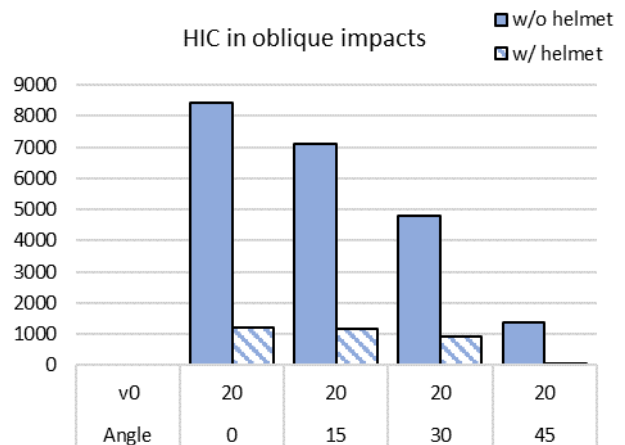
Fig. 6. HIC with and without helmet for different impact angles ($v_0 = 20$ km/h).

In addition to HIC, DAMAGE, using rotational accelerations, was analysed. Values ranged from 0.13 to 0.60 without helmet and from 0.12 to 0.70 with helmet. The maximum value with helmet was obtained at the highest impact velocity of 30 km/h (no matching simulation without helmet). In frontal impacts DAMAGE showed a linear increase (Fig. 7). When increasing the impact angle from 0° to 30°, an almost linear decrease was observed, while the value dropped even further at an angle of 45° (Fig. 8). Those trends were consistent both without and with helmet. DAMAGE with helmet was lower for all simulations, compared to those without helmet. On average, DAMAGE decreased by 16.6% when wearing a helmet (16.1% in frontal impacts; 17.3% in oblique impacts).
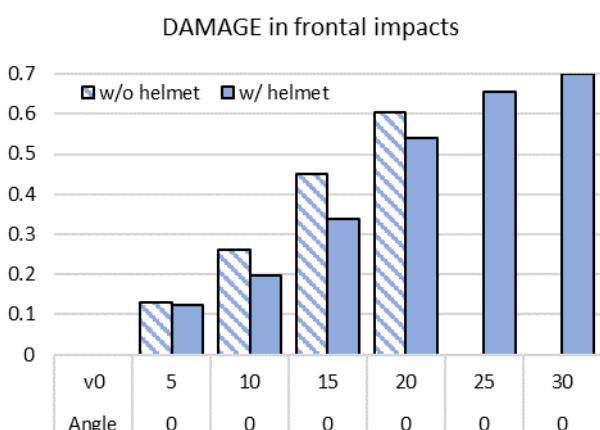

Fig. 7. DAMAGE with and without helmet in frontal impacts (0deg) for different impact velocities; no simulations without helmet were conducted for $v_0 > 20$ km/h.
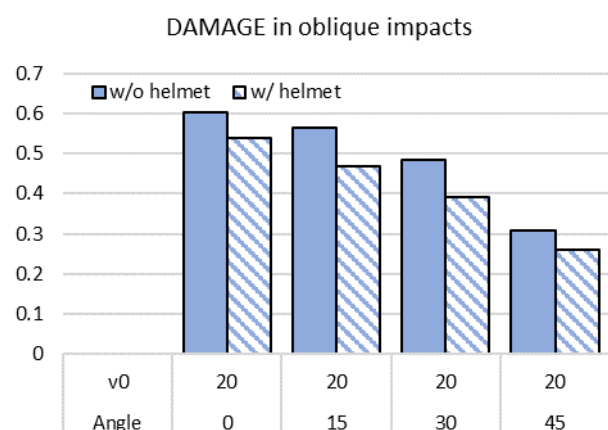
Fig. 8. DAMAGE with and without helmet for different impact angles ($v_0 = 20$ km/h).

Values for 95th MPS in the brain tissue were between 7.8% and 25.9% without helmet and between 7.8% and 31.8% with helmet. The highest value with helmet was observed at 25 km/h (no matching simulation without helmet). The 95th MPS of the brain showed an almost linear increase in frontal impacts when impact velocity increased (Fig. 9). This trend was observed for simulations with and without helmet. For increasing impact angles an almost linear decrease of brain strains was observed (Fig. 10). For all simulations, MPS in the brain was lower when wearing a helmet. The average reduction when wearing a helmet was 9.9% in frontal impacts, 13.1% in oblique impacts and 11.3% overall. At an impact velocity of 5 km/h the difference between with and without helmet was only 0.1%.

The 99th MPS in the skull bone was between 0.45% and 1.45% without helmet (Fig. 11) and between 0.05% and 0.81% with helmet (Fig. 12). In frontal impacts at 10 km/h and 15 km/h without helmet, similar strains in the skull were observed. In an oblique impact at 30° without helmet, the MPS was the skull is rather low, compared to the 15- and 45-degree impact. As for the 95th MPS in the brain, the increasing trend levelled off for a frontal 30 km/h impact (with helmet). Strains in the skull were drastically lower in simulations with helmet (79.2% overall).

Rib strains ranged from approximately 0.6% to 2.5% (Fig. A1, Fig. A2, TABLE A4), increasing with impact velocity

in frontal impacts. In oblique impacts, rib strains decreased with increasing impact angles.

Strains in the femur ranged from 0.1% to 2.8%. Strains in the left femur were drastically increasing in oblique impacts, while the same time strains in the right femur decreased (Fig. A1, Fig. A2, TABLE A4).
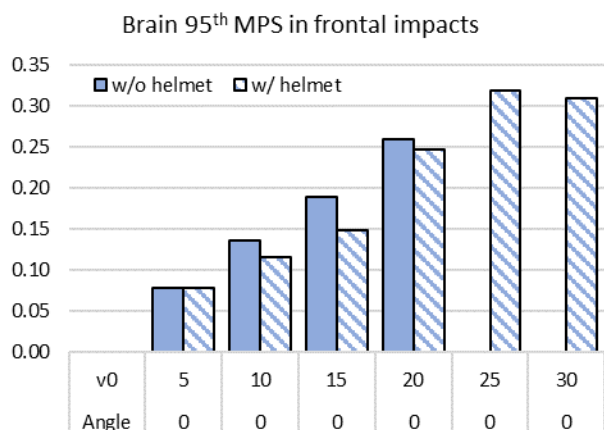
Fig. 9. 95th MPS brain with and without helmet in frontal impacts (0deg) for different impact velocities; no simulations without helmet were conducted for $v_0 > 20$ km/h.
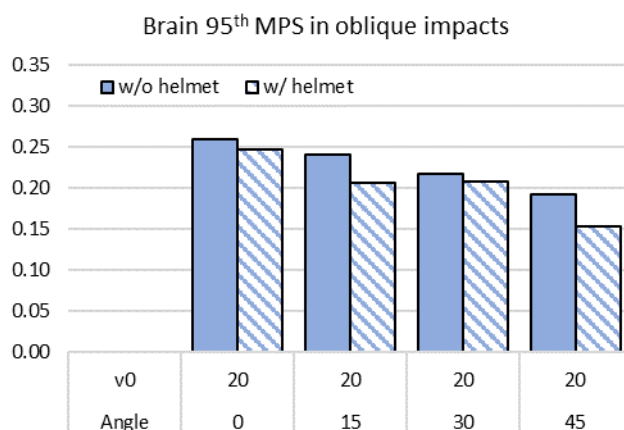
Fig. 10. 95th MPS brain with and without helmet for different impact angles ($v_0 = 20$ km/h).
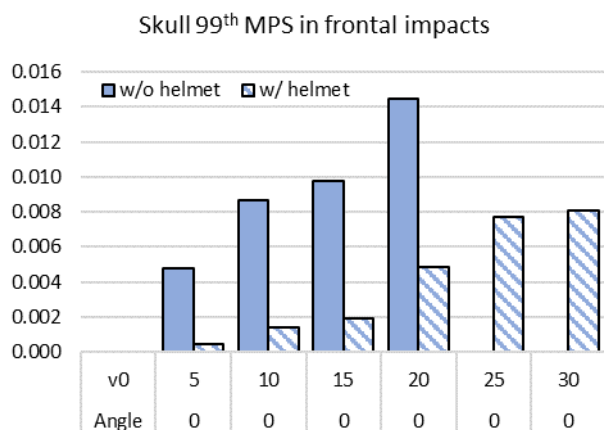
Fig. 11. 99th MPS in the cortical skull with and without helmet in frontal impacts (0deg) for different impact velocities; no simulations without helmet were conducted for $v_0 > 20$ km/h.
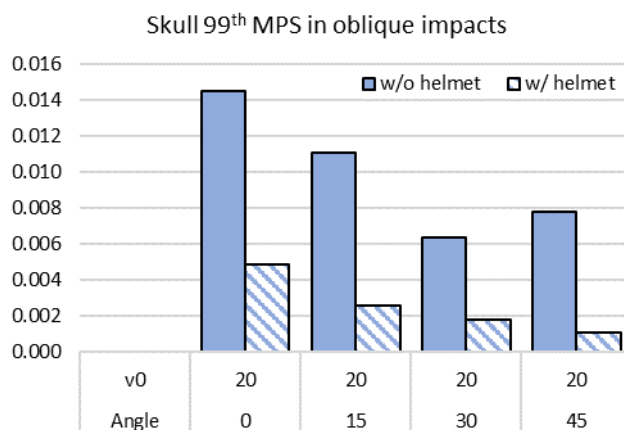
Fig. 12. 99th MPS in the cortical skull with and without helmet for different impact angles ($v_0 = 20$ km/h).

Child and adult riding together

In the case of the child sitting in the front, the child was pushed into the tree by the adult, after the sledge was decelerated. This resulted in increased loading of the femur of the child (Fig. A8, Fig. A9). Subsequently, the head impacted the tree, as in the simulations of the child riding alone. In contrast to those simulations, an excessive head rebound was prevented by the adult's chest. Finally, the adult's head also impacted the tree (Fig. A3, top row).

In the case of the adult sitting at the front, the adult's head experienced a heavy impact at the tree, forcing the head to rebound and the neck to extend heavily. Subsequently, the adult's thorax impacted the tree. Thereafter, the child's head impacted the back of the adult, while the thorax impacted the lower back and hip of the adult at the same time (Fig. A3, bottom row).

Injury criteria child

HIC ranged from 1,013 to 5,634 for the child sitting in the front, and from 162 to 286 when sitting in the rear (>Fig. 13, TABLE A2). In all those simulations, the child was wearing a helmet. The simulation with the child sitting in the rear at 30 km/h and 30° terminated when the adult's thorax impacted the tree (after approximately 115 ms). When analysing the simulation, it was found that the sternal end of the left clavicle was pushing hard against the

soft tissue of the thorax, causing an element of the thoracic fat tissue to fail due to negative volume. Since this error occurred when the thorax compression started and we did not intend to modify the original models, it was only possible to obtain injury values for the adult's head. Values for other body regions of the adult could not be evaluated. Additionally, no values for the child could be obtained for this simulation.

On average, HIC was reduced by 85.4% when the child was sitting behind the adult, while DAMAGE was reduced by approximately 41% (Fig. 14). The effect was stronger for smaller angles (0° and 15°) than for 30°-impacts. Regarding brain strains (Fig. 15), a similar behaviour as for DAMAGE was observed – a stronger reduction for frontal impacts than for oblique impacts. Strain values ranged from 20.0% to 30.4% and 11.8% to 22.5% when the child sat at the front and rear, respectively. The 99th MPS of the skull ranged from 0.6% to 1.3% for the child sitting at the front and from 0.1% to 0.2% when sitting in the rear. Similar to HIC, a strong reduction of skull strains (83%) was observed for the child sitting behind the adult person.
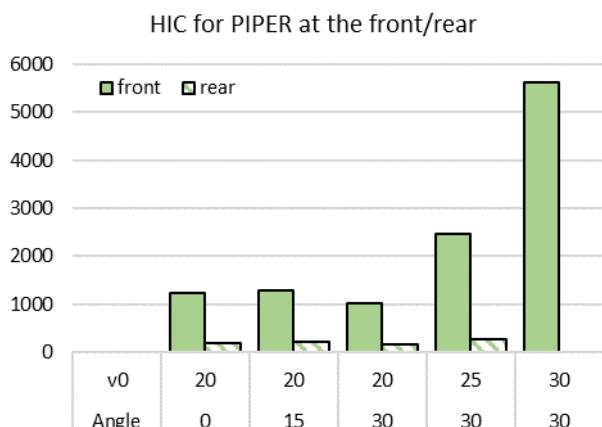
>Fig. 13. HIC for PIPER in the front and rear for different impact angles (v_0 =20 km/h) and one impact at 25 km/h and 30° (with helmet).
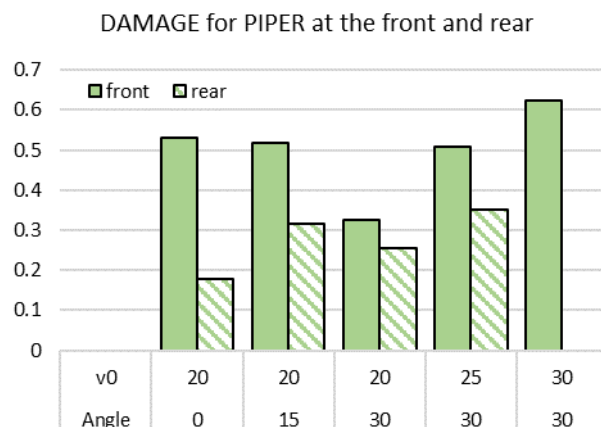

Fig. 14. DAMAGE for PIPER in the front and rear for different impact angles (v_0 =20 km/h) and one impact at 25 km/h and 30° (with helmet).
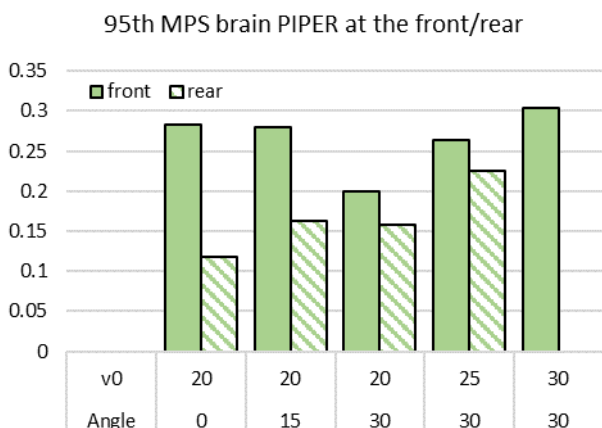

Fig. 15. 95th MPS in the brain for PIPER in the front and rear for different impact angles (v_0 =20 km/h) and one impact at 25 km/h and 30° (with helmet).
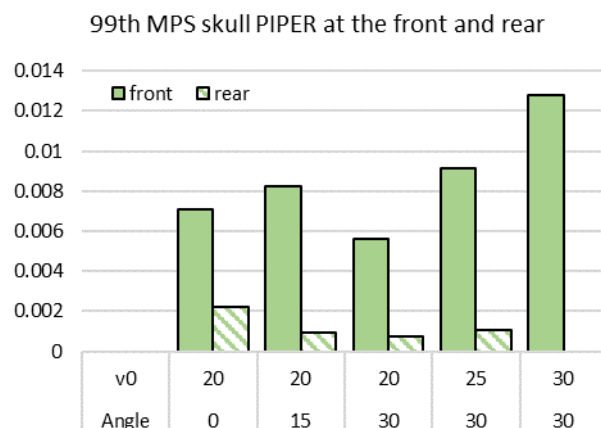

Fig. 16. 99th MPS in the skull for PIPER in the front and rear for different impact angles (v_0 =20 km/h) and one impact at 25 km/h and 30° (with helmet).

Fig. 17 shows the 99th MPS in the cortical ribs and femur of the PIPER model, when riding together with an adult person. Rib strains were similar for frontal and oblique impacts at 20 km/h. Almost no difference between the child sitting at the front and rear occurred.

Similar strains for the left and right femur were observed in frontal collisions (Fig. 17). For the child in the front, strains ranged from 2.0% to 4.3% (left femur) and from 0.9% to 2.2% (right femur). When the child was sitting in the rear, strains ranged from 0.2% to 0.7% for the left femur and 0.4% to 1.3% for the right femur, respectively. When the impact angle was varied, a pronounced asymmetric behaviour was observed, resulting in considerably larger strains in the left femur compared to the right femur. For the left femur, significant differences between the seating positions were observed. All criteria values can be found in the Appendix (TABLE A3).
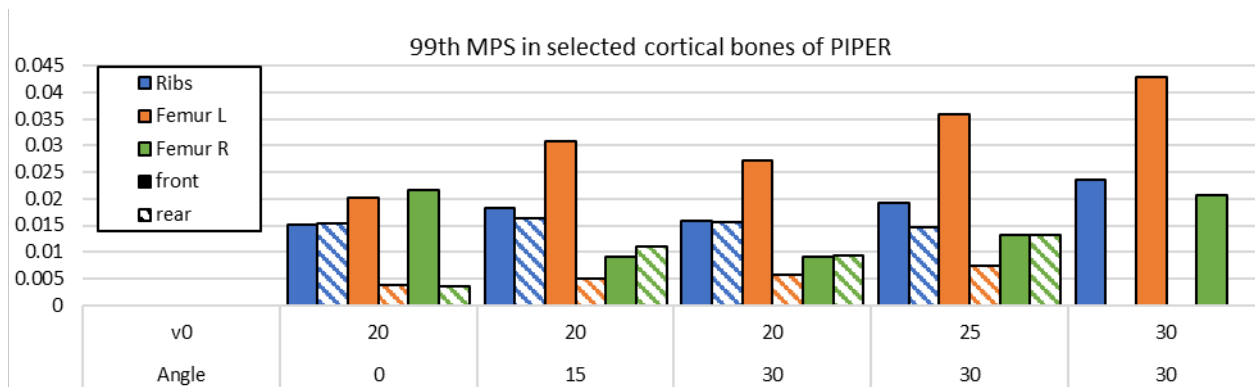
Fig. 17. 99th MPS in cortical ribs and femur for PIPER sitting in the front and the rear. Solid bars representing the child sitting in front, hatched ones representing the child sitting in the rear.

Injury criteria adult

For THUMS, HIC was between 2,236 and 7,297 when sitting behind the child and between 3,205 and 7,114 when sitting at the front (Fig. 18,TABLE A5). Although the HIC of the adult was higher when sitting at the front, it was also high when sitting behind the child, since the head of the adult contacted the tree in all simulations with the adult sitting in the back and no helmet model was used for the adult. However, for the simulation at 25 km/h and 30° the HIC was slightly higher for the THUMS sitting in the rear. In contrast to the child, HIC increased with increasing impact angles (THUMS at the rear).

DAMAGE ranged from 0.42 to 0.86 (rear) and from 0.39 to 0.59 (front, Fig. 19). Observed DAMAGE values were almost identical, regardless of the seating position of the THUMS and the impact angle. Only for higher impact velocities DAMAGE did increase.
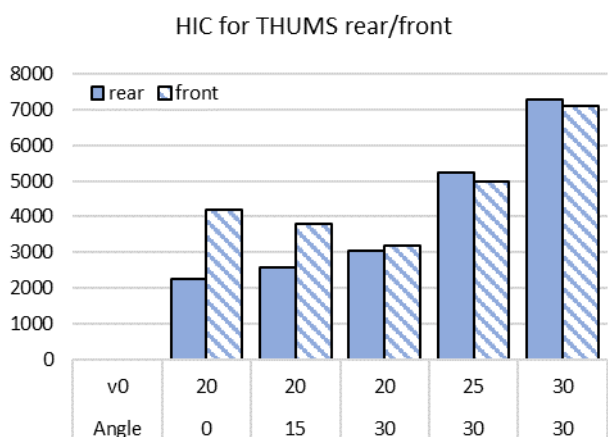

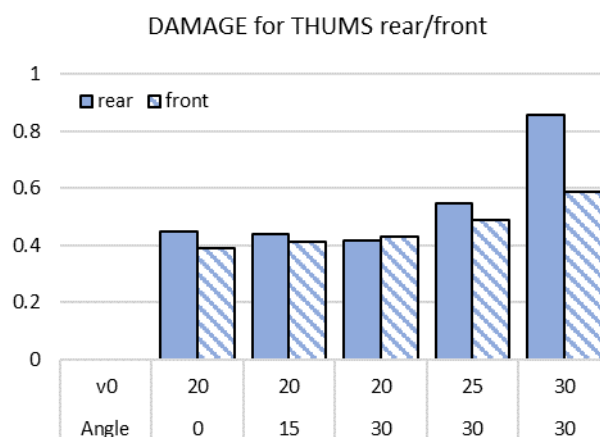Fig. 18. HIC for THUMS in different positions on the sled.

Fig. 19. DAMAGE for THUMS in different positions on the sled.

Regarding the 95th MPS in the brain (Fig. 20), a different trend was observed compared to the other metrics. For an adult sitting in the rear, almost no change in brain MPS was observed for different impact angles at 20 km/h, while it increased for higher impact velocities. MPS in the brain was larger when sitting at the front, except the simulations at 20 km/h and 15° and at 30 km/h and 30°.

The behaviour observed for the 99th MPS of the skull is more or less consistent with HIC (Fig. 21). All values were larger when sitting in the front. An almost linear increase for increasing impact angles was observed for the adult in the rear, while a decreasing trend was present when sitting in the front.

For the ribs as well as the left clavicle, higher strains occurred when the THUMS was sitting in front of the child, while strains in the right clavicle were higher, when THUMS was sitting in the rear (TABLE A8), since THUMS impacted the helmet of the child when sitting at the rear.
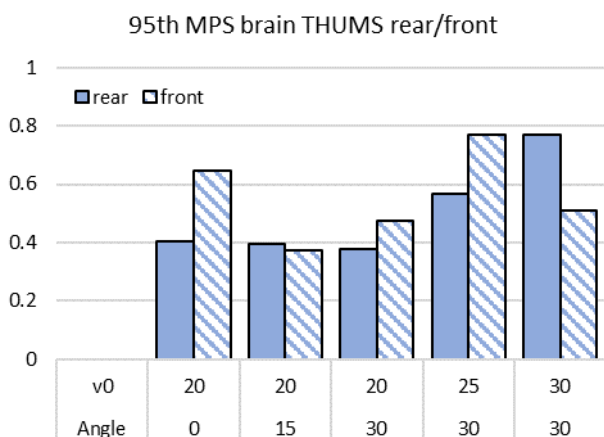
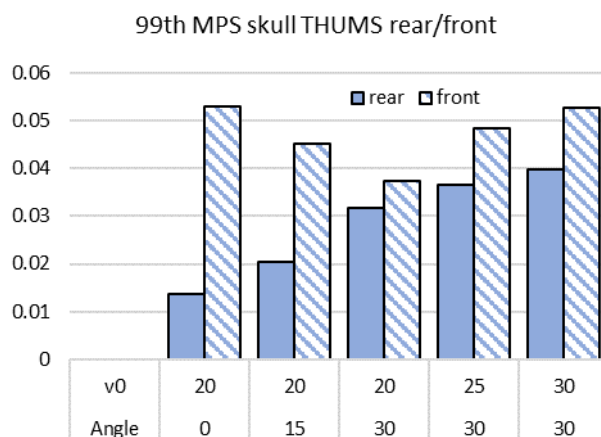Fig. 20. 95th MPS brain for THUMS in different positions on the sled.

Fig. 21. 99th MPS skull for THUMS in different positions on the sled.

IV. DISCUSSION

To the author's best knowledge, this is the first study to investigate sledging-related accidents by means of Finite Element Analysis using HBMs. The accident analysis showed that sledging is a potentially dangerous activity, leading to a significant number of sledging related injuries in Austria. While adults account for the largest proportion of injured people, the share of children and adolescents is similar. Collisions turned out to be amongst the most frequent accident scenarios, especially the ones involving major trauma. Therefore, a collision with a tree was further investigated in this study.

Effect of helmet

The protective effect of the helmet was stronger for HIC and MPS in the skull, compared to DAMAGE and MPS in the brain. When the child was riding alone, large reductions of HIC and skull strains were obtained when wearing a helmet. Already at an impact velocity of 10 km/h, a significant benefit of the helmet was observed. The resultant linear head acceleration for the frontal 10 km/h impact with and without helmet is shown in Fig. 22. While the impact caused accelerations of almost 250 g without helmet, the maximum acceleration with helmet was only about 100 g, as energy is absorbed over a longer duration, using the deformation area of the helmet. As the initial position of the head relative to the tree was the same for simulations with and without helmet, the helmet to tree contact occurred slightly earlier when wearing a helmet, explaining the shift of the acceleration peak (Fig. 22).

Without helmet, a HIC of 1,218 occurred at a relatively low impact velocity of 10 km/h (frontal impact). In comparison, a similar HIC (1,184) was obtained in a frontal, 20 km/h impact when wearing a helmet. Nevertheless, head trauma may still occur at higher impact velocities despite wearing a helmet. No clear threshold can be stated, as no validated model-specific injury risk curves are available now. Furthermore, the threshold up to which velocity the helmet is effective is supposed to depend on the specific helmet model.
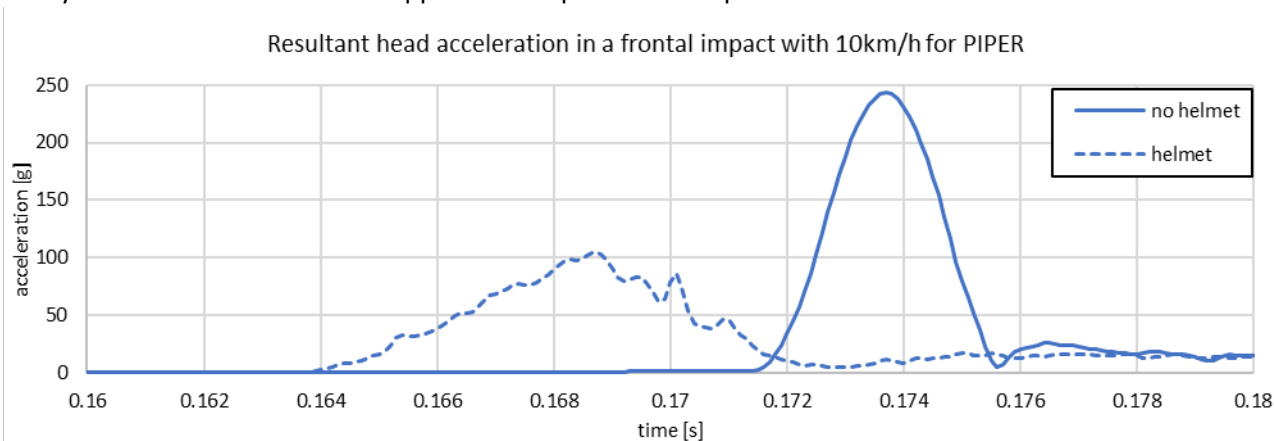

Fig. 22. Resultant head acceleration (CFC1000) for a frontal, 10 km/h impact of the child without and with helmet. Time axis was clipped to the time of the head impact.

When taking a closer look at the head impact, only a small amount of relative motion between head and helmet was observed. The helmet used in this study did not contain any specific protection addressing rotational injuries, such as MIPS (Multi-Directional Impact Protection System). Helmets including such systems might be able to reduce these metrics more effectively than the helmet used in this study. Nevertheless, all evaluated head injury metrics were reduced when introducing the helmet model in the simulations.

It must be mentioned that the helmet model used in this study is a bicycle and not a skiing helmet. Although the general shape of this specific bicycle helmet seems to be representative for a skiing helmet also, a skiing helmet can be even thicker and therefore the protective effect might be higher, compared to the analysed helmet. Since the focus of this research was on the protective effect of helmets in general and not on the development of one specific helmet, this approach seems reasonable. Furthermore, the helmet model used in this study was thoroughly validated and used in previous studies of Klug et al. [20] and Feist and Klug [21]. Furthermore, it was not possible to create a model of a skiing helmet of similar validation quality as the used bicycle helmet, within the framework of this study.

Effect of impact configuration

Within this study, frontal and oblique impacts at an almost rigid obstacle were investigated. When considering head injuries, frontal and oblique impacts at relatively small angles of 15° were found to be more harmful compared to oblique impacts at higher angles (30° and 45°). In contrast, the load on the femur increased for increasing impact angles due to asymmetric loading of the femur. For the child and adult riding together, even more load was applied to the femur since the child's femur got stuck between the sledge, the adult, and the tree (Fig. A8, Fig. A9).

In frontal impacts, HIC showed an exponential increase, while DAMAGE showed an almost linear increase for the PIPER model. The different trend between HIC and DAMAGE is related to their definition. While HIC uses linear accelerations [24], DAMAGE uses rotational accelerations [25]. Brain strains showed a similar behaviour as DAMAGE, which is plausible as DAMAGE was developed to correlate with brain strains, although different HBM was used for the development of DAMAGE [25].

When considering oblique impacts, all head criteria of the PIPER model decreased as the impact angle increased. As a frontal and oblique collision with 15° were similar (Fig. A5), head injury values were also similar for those cases. The trajectory of the head CoG and more detailed explanations of the head kinematics can be found in the Appendix (Fig. A5).

Effect of seating position

In our accident scenario, the rear position was clearly beneficial for the child since injury metrics for the head and femur were lower in this configuration. Regarding rib strains, almost no differences occurred.

HIC values for the child sitting in the front were comparable to those of the child riding alone (with helmet). This is plausible and indicates that impacting the tree initially is more severe than hitting the adult's chest during head rebound.

The interaction between the femur and the sledge was highly affected by the interaction with the adult. While the loads on the femur increased drastically in the case of the adult person sitting behind the child, compared to the child riding alone, the loads on the femur were reduced drastically when the child was sitting behind the adult. A more detailed description of the interaction between the child, the adult person and sledge is provided in the Appendix (Fig. A8, Fig. A9).

Surprisingly, there was almost no reduction of rib strains for the child sitting in the rear. Nevertheless, a different loading pattern of the thorax was observed. While the uppermost ribs experienced higher strains when sitting at the front (Fig. A10), the child seated in the rear was subjected to an increased loading of the 2nd, 6th and 7th rib (Fig. A11), meaning a more uniform chest compression occurred. However, to our knowledge the stiffness of the lower back of THUMS is, not validated for direct impacts, so those results should be taken with caution.

As the other criteria were also reduced, it can be recommended to seat the child behind an adult person when riding together, especially when obstacles (trees, lift poles, etc.) are within proximity of the slope.

Although our findings indicate that children should be seated behind an adult person when riding together, we also know, that this approach might have some other drawbacks, which we have not considered in our study. Smaller children may fall off the sledge (e.g. when going over bumps) and the view of the child is limited when sitting at the rear. Nevertheless, we think that this is the better option, especially when riding within proximity of

stationary objects like trees. On dedicated sledging slopes without stationary obstacles and sufficient run-off areas it may be fine for the child to sit at the front since the risk of a collision is significantly lower. Furthermore, we recommend this setup (child in the rear) only for older children that can hold on to the sledge or the adult properly, reducing the risk of falling off the sledge. Riding together with very small children on steep slopes who cannot hold themselves is anyway not recommended from our perspective. For low-speeds or if the small child is sledging alone, dedicated backrests are available. Nevertheless, the seating setup we recommend is suitable for the type of collision we investigated within this study and considering the age of the child in our simulation.

Influence of head acceleration signals at the PIPER model

When using the original local sensor definition of the PIPER model at the head CoG, very high peak accelerations were observed for some simulations, resulting in high HIC values. When analysing this in detail, it was found that those were caused by the sensor definition for the local head acceleration. The original definition in the PIPER model uses a *CONSTRAINED_EXTRA_NODES keyword, connecting the local coordinate system positioned at the geometric centre of the skull (rigid beams) to some nodes of the outer skull bone (deformable). Hence, there were areas of the skull that were particularly stiff, causing very high head accelerations if the head impact occurred close to those nodes. To make simulation results more robust for our load case, the constraint was changed to an interpolation constraint.

Comparison of head injury criteria of THUMS and PIPER models

TABLE I shows head injury criteria for a frontal 20 km/h collision of PIPER and THUMS. PIPER was riding alone (without helmet), while THUMS was sitting at the front (also without helmet) to make results comparable. The resultant head velocities at time of impact were almost identical: 5.94m/s for PIPER and 5.92m/s for THUMS. Nevertheless, the resulting head injury metrics were different. While HIC and DAMAGE were significantly higher for PIPER, strains in the brain and skull were considerably larger in THUMS.

TABLE I
COMPARISON OF HEAD INJURY CRITERIA FOR A FRONTAL IMPACT AT 20 KM/H
PIPER RIDING ALONE WITHOUT HELMET; THUMS SITTING AT THE FRONT (WITHOUT HELMET)

	HIC	DAMAGE	95th MPS brain	99th MPS skull
PIPER riding alone, without helmet	8,415	0.60	0.259	0.015
THUMS at the front, without helmet	4,193	0.39	0.645	0.053

Those differences might have anthropometric reasons but may also be caused by different modelling approaches. For example, there are differences regarding skull modelling between the HBMs. The skull of PIPER consists of one solid layer, representing the trabecular bone, covered by one layer of shells (thickness: 1 mm) on the in- and outside of the trabecular skull, forming the cortical bone. Like PIPER, THUMS uses one solid layer representing the trabecular bone, covered by one layer of shells (cortical bone) on the in- and outside of the trabecular bone but uses a thickness of 1.5 mm for the cortical bone. Pictures of undeformed as well as the deformed skull are given in the Appendix (Fig. A12, Fig. A13, Fig. A14, Fig. A15). Those relate to a frontal, 20 km/h impact of PIPER (riding alone, without helmet) and THUMS sitting in the front, without helmet, respectively. While the skull of PIPER showed only marginal deformations, the frontal skull bone of THUMS showed significant deformations. This behaviour may lead to a decrease of head accelerations and therefore decreased values of the kinematic criteria (HIC, DAMGE) for THUMS, while strains in the brain and skull were higher in THUMS, compared to PIPER (TABLE I).

Giordano and Kleiven [28] defined the material properties of the brain tissue in the PIPER model based on test data from adult specimen. However, the PIPER brain is modelled using a nonlinear viscoelastic material (*MAT_OGDEN_RUBBER), while the brain of the THUMS uses *MAT_KELVIN-MAXWELL_VISCOELASTIC.

While white and grey matter is distinguished in terms of material properties for THUMS, a homogenous brain matter is modelled in PIPER

Therefore, it can be concluded that results from the adult are not directly comparable to those of the child, as the models differ significantly.

Limitations

The present study underlies several limitations, which are summarised in the following section.

The conclusions are based on a limited number of simulations. Only one type of accident scenario was investigated, representing a worst-case scenario (impacting an almost rigid obstacle). We chose this specific scenario since we found from our accident data as well as from existing literature, that collisions with stationary objects frequently lead to major trauma. Additionally, only the impact at the obstacle and no subsequent ground impact was simulated. The simulation of the ground impact is particularly difficult since more information on slope conditions (e.g. ice) and other obstacles surrounding the accident site are needed.

The sledge was modelled rigid and not validated. A failure of the sledge could potentially influence the occupant kinematics prior to the impact at the obstacle. However, no data on failure of the sledge was available from our accident data or existing literature focussing on sledging accidents. Future research could include crash testing of sledges to derive a validated sledge model, capable of predicting failure and leading to more detailed insights in sledging injuries.

No muscle activity was implemented in the used HBMs. Therefore, no pre-crash reactions were considered. Realistically, we would expect some accident avoidance manoeuvre, like attempting to turn or to brake, influencing both impact location at the obstacle and impact velocity. Additionally, we defined typical positions of the riders on the sledge to the best of our knowledge. Future research could include studies using videos analysis to identify realistic seating positions, accident avoidance manoeuvres and typical riding velocities. This input could be used to refine the simulation setup and derive improved conclusions.

Although heavy extensions of the neck were observed for both occupants (PIPER and THUMS) and neck injuries resulting from sledging accidents are mentioned in literature [3], [5], [13], no neck injury criteria were evaluated in this study. The focus of this study was on the effect of the helmet and the seating position for which we suspected other body regions (head, thorax, and lower extremities) to be more relevant.

A major limitation of the interpretation of results is the lack of validated injury risk curves for the applied models. Generally, literature on strain limits of paediatric cortical bone is limited. While the papers of Yasuki and Yamamae [29] and Golman *et al.* [30] use a strain threshold of 1.5% as indicator for cortical bone fracture, the publications of Currey and Butler [31] and Ivarsson *et al.* [32] suggest a limit of 0.8%. Applying a limit of 0.8 % to our simulation leads to a prediction of rib fractures in seven out of nine cases of the child riding alone (with helmet), while the 1.5% strain results in the prediction of only three cases. For the simulations, in which the child sits in front of the adult person, the strain limit would not make a difference, since rib strains are higher than 1.5% in all these simulations.

V. CONCLUSIONS

Within this study the effect of helmet usage and different seating positions was investigated in one specific sledging accident scenario, leading to the following conclusions.

- Our simulations indicate that wearing a helmet can significantly reduce the risk of head injury in collisions, even at impact velocities as low as 10 km/h. This trend was observed for all evaluated head injury metrics, although different levels of improvement were found for criteria resulting from linear versus rotational accelerations.
- Frontal impacts were more harmful to the head, while the lower extremities (femur) were at higher risk of injury in oblique impacts.
- Under the crash conditions studied here, it is safer for the child to ride in the back. In our simulations loads on the head and femur were reduced significantly in this configuration.

VI. ACKNOWLEDGEMENTS

VII. REFERENCES

[1]   Ruedl, G., Pocecco, E., *et al.* (2017) Unfallursachen und Risikofaktoren bei erwachsenen Rodlern: eine retrospektive Studie. *Sportverletzung Sportschaden Organ der Gesellschaft fuer Orthopaedisch-Traumatologische Sportmedizin*, **31**(1): pp.45–49.

[2]   Regan, L. A., Cooper, J. G. (2011) Sledging is still a seasonal source of serious injury in Scottish children. *Scottish medical journal*, **56**(4): pp.188–190.

[3]   Noffsinger, D., Nuss, K., Haley, K., Ford, N. (2008) Pediatric sledding trauma: avoiding the collision. *Journal of Trauma Nursing*, **15**(2): pp.58–61.

[4]   Corra, S., de Giorgi, F. (2007) Sledding injuries: is safety in this winter pastime overlooked? A three-year survey in South-Tyrol. *Journal of Trauma Management & Outcomes*, **1**(1): p.5.

[5]   Skarbek-Borowska, S., Amanullah, S., Mello, M. J., Linakis, J. G. (2006) Emergency department visits for sledding injuries in children in the United States in 2001/2002. *Academic Emergency Medicine*, **13**(2): pp.181–185.

[6]   Federiuk, C. S., Schlueter, J. L., Adams, A. L. (2002) Skiing, Snowboarding, and Sledding Injuries in a Northwestern State☆. *Wilderness & Environmental Medicine*, **13**(4): pp.245–249.

[7]   Voaklander, D. C., Kelly, K. D., Sukrani, N., Sher, A., Rowe, B. H. (2001) Sledding injuries in patients presenting to the emergency department in a northern city. *Academic emergency medicine official journal of the Society for Academic Emergency Medicine*, **8**(6): pp.629–635.

[8]   Verrees, M., Robinson, S., Cohen, A. R. (2004) Sledding accidents in children: potential for serious injury, risk of fatality. *Pediatric Neurosurgery*, **40**(1): pp.2–7.

[9]   Herman, R., Hirschl, R. B., Ehrlich, P. F. (2015) Sledding injuries a practice-based study is it time to raise awareness? *Pediatric surgery international*, **31**(3): pp.237–240.

[10]   Sloan, J. P., Maheson, M., Dove, A. F. (1985) How dangerous is sledging? *British medical journal* (Clinical research ed.), **290**(6471): p.821.

[11]   Rowe, B. H., Bota, G. W. (1994) Sledding deaths in Ontario. *Canadian Family Physician*, **40**: pp.68–71.

[12]   Cimpello, L. B., Garcia, M., Rueckmann, E., Markevicz, C. (2009) Sledding: how fast can they go? *The Journal of trauma*, **663**(SupplS23-6).

[13]   Ortega, H. W., Shields, B. J., Smith, G. A. (2005) Sledding-related injuries among children requiring emergency treatment. *Pediatric Emergency Care*, **21**(12): pp.839–843.

[14]   Hackam, D. J., Kreller, M., Pearl, R. H. (1999) Snow-related recreational injuries in children: Assessment of morbidity and management strategies. *Journal of Pediatric Surgery*, **34**(1): pp.65–69.

[15]   Major, C. P., Guest, D. P., Smith, L. A., Barker, D. E., Burns, R. P. (1999) Sledding injuries in the southeastern United States. *Southern Medical Journal*, **92**(2): pp.193–196.

[16]   Shorter, N. A., Mooney, D. P., Harmon, B. J. (1999) Childhood sledding injuries. *The American Journal of Emergency Medicine*, **17**(1): pp.32–34.

[17]   Jost, B. "Baumalter bestimmen", https://www.baumportal.de/baum-alter-bestimmen [Accessed 21 January 2021].

[18]   Murray, Yvonne D. (2007) Manual for LS-DYNA wood material model 143, 6300 Georgetown Pike McLean, VA 22101-2296.

[19]   Murray, Yvonne D., Reid, J. D., Faller, R. K., Bielenberg, B. W., Paulsen, T. J. (2005) Evaluation of LS-DYNA Wood Material Model 143, 6300 Georgetown Pike McLean, VA 22101-2296.

[20]   Klug, C., Feist, F., Tomasch, E. (2015) Testing of bicycle helmets for preadolescents. *Proceedings of IRCOBI Conference*, 2015, Lyon, France.

[21]   Feist, F., Klug, C. (2016) A Numerical Study on the Influence of the Upper Body and Neck on Head Kinematics in Tangential Bicycle Helmet Impact. *Proceedings of IRCOBI Conference*, 2016, Malaga, Spain.

[22]   DIN EN 1078:2014-04, Helme für Radfahrer und für Benutzer von Skateboards und Rollschuhen; Deutsche Fassung EN_1078:2012+A1:2012, Berlin.

[23]   DIN 32912:2019-12, Schilder für den organisierten Skiraum_- Anforderungen, Ausführung und Klassifizierung, Berlin.

[24]   Versace, J. (1971) A Review of the Severity Index. *Proceedings of Stapp Car Crash Conference*, 1971, Coronado, CA.

[25]   Gabler, L. F., Crandall, J. R., Panzer, M. B. (2019) Development of a Second-Order System for Rapid Estimation of Maximum Brain Strain. *Annals of Biomedical Engineering*, **47**(9): pp.1971–1981.

[26]   SAE J211-1: Instrumentation for Impact Test; SAE International

[27]   Schachner, M., Micorek, J., Luttenberger, P., Greimel, R., Klug, C. "Dynasaur", https://gitlab.com/VSI-TUGraz/Dynasaur.

[28]   Giordano, C., Kleiven, S. (2016) Development of a 3-Year-Old Child FE Head Model, Continuously Scalable from 1.5- to 6- Year-Old. *Proceedings of IRCOBI Conference,* 2016, Malaga, Spain.

[29]   Yasuki, T., Yamamae, Y. (2010) Validation of Kinematics and Lower Extremity Injuries Estimated by Total Human Model for Safety in SUV to Pedestrian Impact Test. *Journal of Biomechanical Science and Engineering*, **5**(4): pp.340–356.

[30]   Golman, A. J., Danelson, K. A., Miller, L. E., Stitzel, J. D. (2014) Injury prediction in a side impact crash using human body model simulation. *Accident analysis and prevention*, **64**: pp.1–8.

[31]   Currey, J. D., Butler, G. (1975) The mechanical properties of bone tissue in children. T*he Journal of bone and joint surgery*, American volume, **57**(6): pp.810–814.

[32]   Ivarsson, B. J., Crandall, J. R., Longhitano, D., Okamoto, M. (2004) Lateral Injury Criteria for the 6-year-old Pedestrian – Part II: Criteria for the Upper and Lower Extremities. 2004 SAE World Congress SAE/SP-1801.

VIII. APPENDIX

TABLE A1
SIMULATION MATRIX

| Group | # | Impact conditions | | Occupants | | | |
| | | v_0 [km/h] | Angle [°] | Front seat | | Rear seat | |
				Person	Helmet	Person	Helmet
Group 1 - Child without helmet	1	5	0	Child	no	-	-
	2	10	0				
	3	20	0				
	4	20	15				
	5	20	30				
	6	20	45				
Group 2 - Child with helmet	7	5	0	Child	yes	-	-
	8	10	0				
	9	15	0				
	10	20	0				
	11	20	15				
	12	20	30				
	13	20	45				
	14	25	0				
	15	30	0				
Group 3 - Child at front seat	16	20	0	Child	yes	Adult	no
	17	20	15				
	18	20	30				
	19	25	30				
	20	30	30				
Group 4 - Child at rear seat	21	20	0	Adult	no	Child	yes
	22	20	15				
	23	20	30				
	24	25	30				
	25	30	30				

TABLE A2
PARTS INCLUDED IN PIPER STRAIN EVALUATION

Body region	Component	Part ID	Part Name
Head	Skull	1110	HE_BO_ExternalTable
	Brain	1500	HE_OR_Cerebral_Cortex
		1501	HE_OR_Cerebellum
Thorax	Sternum	4112	TX_BO_Sternum_2D
	Ribs	4113	TX_BO_Ribs_2D
	Right Clavicle	4138	TX_BO_R_Clavicle_2D
	Left Clavicle	4139	TX_BO_L_Clavicle_2D
Upper Extremities	Left Humerus	3102	UX_BO_L_Humerus_2D
		3103	UX_BO_L_HumerusEmphysisProximal_3D
	Right Humerus	5102	UX_BO_R_Humerus_2D
		5103	UX_BO_R_HumerusEmphysisProximal_3D
Lower Extremities	Left Femur	7102	LX_BO_L_FemurMetaphysisProximal_2D
		7103	LX_BO_L_FemurDiaphysis_2D
		7104	LX_BO_L_FemurMetaphysisDistal_2D
	Right Femur	9102	LX_BO_R_FemurMetaphysisProximal_2D
		9103	LX_BO_R_FemurDiaphysis_2D
		9104	LX_BO_R_FemurMetaphysisDistal_2D
	Left Tibia	7123	LX_BO_L_TibiaDiaphysis_2D
	Right Tibia	9123	LX_BO_R_TibiaDiaphysis_2D
	Left Fibula	7133	LX_BO_L_FibulaDiaphysis_2D
	Right Fibula	9133	LX_BO_R_FibulaDiaphysis_2D

The following code sequence shows the definition of DAMAGE in the open-source post-processing tool Dynasaur [27]. In this case the rotational accelerations of the head are filtered (CFC1000) as recommended in [26]. Then DAMAGE is calculated as described in [25], using the constants defined in the code section below.

```
# Evaluation of DAMAGE
{
  "CRITERIA": [
    { "name": "DAMAGE",
     "type_of_criteria": "injury",
      "part_of": "HEAD",
      "function": {
        "name": "DAMAGE",
         "param": {
           "ra_x": {"function": { "name": "cfc", "param": { "cfc": 1000, "time": {"type": "NODE", "ID": "Head",
           "array": ["(0, time)"]}, "sampled_array": {"type": "NODE", "ID": "Head", "array": ["(0,
           rx_acceleration)"]}}}},
           "ra_y": {"function": { "name": "cfc", "param": { "cfc": 1000, "time": {"type": "NODE", "ID": "Head",
           "array": ["(0, time)"]}, "sampled_array": {"type": "NODE", "ID": "Head", "array": ["(0,
           ry_acceleration)"]}}}},
           "ra_x": {"function": { "name": "cfc", "param": { "cfc": 1000, "time": {"type": "NODE", "ID": "Head",
           "array": ["(0, time)"]}, "sampled_array": {"type": "NODE", "ID": "Head", "array": ["(0,
           ry_acceleration)"]}}}},
           "time": {"type": "NODE", "ID": "Head", "array": ["(0, time)"]},
           "mx": 1,
           "my": 1,
           "mz": 1,
           "kxx": 32142,
           "kyy": 23493,
           "kzz": 16935,
           "kxy": 0,
           "kyz": 0,
           "kxz": 1636.3,
           "a0": 0,
           "a1": 0.0059148,
           "beta": 2.9903
         }
       }
     }
   ]
}
```

The following code sequence shows how the 95th MPS of the brain was evaluated using the open-source post-processing tool Dynasaur [27]. First, the object "Brain" consisting of several individual parts was defined. Then the time histories of the strains included in the object "brain" were read and stored for all time steps before the 95th percentile strain was computed and returned.

```
# Object Definition of the Brain
{
   "OBJECTS": [
     {
       "type": "OBJECT",
         "name": "Brain",
         "id": [1500, 1501]
     }
   ]
}
# Evaluation of 95th MPS in the Brain
{
   "CRITERIA": [
     {
       "name": "Brain_95p",
         "type_of_criteria" : "injury",
         "part_of" : "BRAIN",
         "function": {
           "name": "percentile",
           "param": {
             "object_data":{
               "type" : "OBJECT",
               "ID" : "Brain",
               "strain_stress": "Strain"
             },
             "integration_point": "Mean",
             "selection_tension_compression": "Overall",
             "percentile": 0.95
           }
         }
     }
   ]
}
```

TABLE A3

HEAD INJURY CRITERIA FOR PIPER WITHOUT AND WITH HELMET

Impact Parameters		HIC		DAMAGE		Brain MPS 95th		Skull MPS 99th	
v_0	Angle	Helmet		Helmet		Helmet		Helmet	
[km/h]	[deg.]	no	yes	no	yes	no	yes	no	yes
5	0	166	23	0.13	0.12	0.078	0.078	0.0048	0.0005
10	0	1218	210	0.26	0.20	0.136	0.116	0.0087	0.0014
15	0	3773	522	0.45	0.34	0.189	0.149	0.0098	0.0019
20	0	8415	1197	0.60	0.54	0.259	0.247	0.0145	0.0049
20	15	7090	1184	0.57	0.47	0.241	0.207	0.0111	0.0026
20	30	4814	925	0.49	0.39	0.217	0.208	0.0064	0.0018
20	45	1364	79	0.31	0.26	0.193	0.153	0.0078	0.0011
25	0	-	3029	-	0.66	-	0.318	-	0.0077
30	0	-	7807	-	0.70	-	0.309	-	0.0081

TABLE A4
99TH MPS FOR SELECTED CORTICAL BONES OF PIPER RIDING ALONE

Impact Parameters		Ribs		Femur L		Femur R	
v_0	Angle	Helmet		Helmet		Helmet	
[km/h]	[deg]	no	yes	no	yes	no	yes
5	0	0.006	0.006	0.001	0.002	0.001	0.002
10	0	0.007	0.007	0.005	0.005	0.005	0.005
15	0	0.012	0.011	0.007	0.007	0.007	0.007
20	0	0.018	0.015	0.012	0.012	0.013	0.013
20	15	0.016	0.015	0.023	0.025	0.007	0.007
20	30	0.012	0.012	0.014	0.013	0.007	0.007
20	45	0.011	0.010	0.027	0.034	0.008	0.010
25	0	-	0.019	-	0.024	-	0.023
30	0	-	0.025	-	0.031	-	0.034
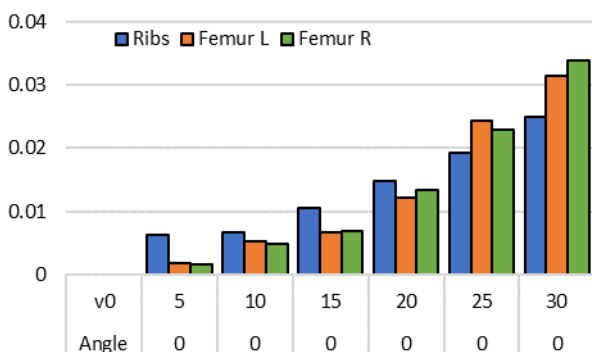
Fig. A1. 99th MPS in the cortical ribs and femur frontal impacts (0deg, with helmet) for different impact velocities.
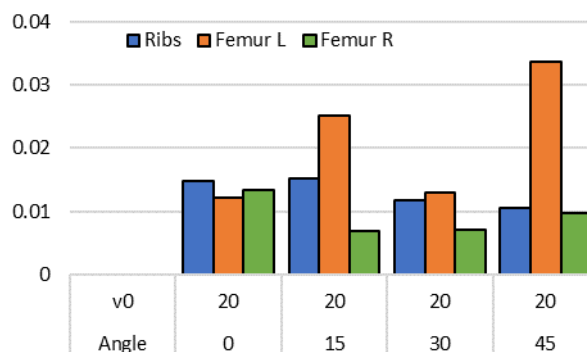
Fig. A2. 99th MPS in the cortical ribs and femur for different impact angles (v_0 = 20 km/h, with helmet).
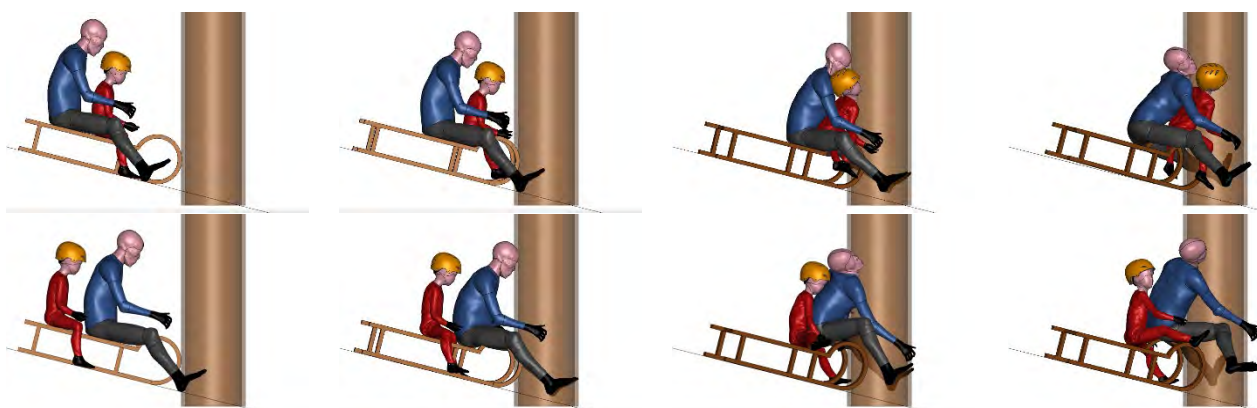

Fig. A3. Impact sequence of the child and an adult riding together. Top row: child sitting in the front; Bottom row child sitting in the rear; Impact velocity: 20 km/h; Impact angle 30°; Pictures representing times of 40 ms, 100 ms, 160 ms and 220 ms, respectively.

TABLE A5
HEAD INJURY CRITERIA FOR PIPER SITTING AT THE FRONT/REAR (WITH HELMET)

Impact Parameters		HIC		DAMAGE		Brain 95th MPS		Skull MPS 99th	
v_0	Angle	Position		Position		Position		Position	
[km/h]	[deg.]	front	rear	front	rear	front	rear	front	rear
20	0	1228	195	0.53	0.18	0.283	0.118	0.007	0.002
20	15	1289	209	0.52	0.32	0.279	0.164	0.008	0.001
20	30	1013	162	0.36	0.26	0.200	0.159	0.006	0.001
25	0	2479	257	0.51	0.35	0.264	0.225	0.009	0.001
30	0	5634	*	0.62	*	0.304	*	0.013	*

*no value could be obtained since an error termination occurred.

TABLE A6
99TH MPS FOR SELECTED CORTICAL BONES OF THE PIPER WHEN RIDING WITH AN ADULT PERSON

Impact Parameters		Ribs		Femur L		Femur R	
v_0	Angle	Position		Position		Position	
[km/h]	[deg.]	front	rear	front	rear	front	rear
20	0	0.015	0.015	0.020	0.004	0.022	0.004
20	15	0.018	0.016	0.031	0.005	0.009	0.011
20	30	0.016	0.016	0.027	0.006	0.009	0.009
25	30	0.019	0.015	0.036	0.007	0.013	0.013
30	30	0.024	*	0.043	*	0.021	*

*no value could be obtained since an error termination occurred.

TABLE A7
HEAD INJURY CRITERIA FOR THUMS SITTING AT THE REAR/FRONT

Impact Parameters		HIC		DAMAGE		Brain MPS 95th		Skull MPS 99th	
v_0	Angle	Position		Position		Position		Position	
[km/h]	[deg.]	rear	front	rear	front	rear	front	rear	front
20	0	2236	4193	0.45	0.39	0.403	0.645	0.014	0.053
20	15	2587	3794	0.44	0.41	0.396	0.375	0.020	0.045
20	30	3053	3205	0.42	0.43	0.379	0.473	0.032	0.037
25	30	5241	4976	0.55	0.49	0.566	0.768	0.037	0.049
30	30	7297	7114	0.86	0.59	0.772	0.511	0.040	0.053

TABLE A8
99TH MPS IN SELECTED CORTICAL BONES OF THUMS SITTING AT THE REAR/FRONT

Impact Parameters		Ribs		Clavicle L		Clavicle R	
v_0	Angle	Position		Position		Position	
[km/h]	[deg.]	front	rear	front	rear	front	rear
20	0	0.006	0.009	0.014	0.006	0.014	0.006
20	15	0.004	0.008	0.004	0.012	0.011	0.004
20	30	0.004	0.007	0.008	0.036	0.008	0.004
25	30	0.006	0.011	0.032	0.050	0.010	0.007
30	30	0.006	*	0.062	*	0.009	*

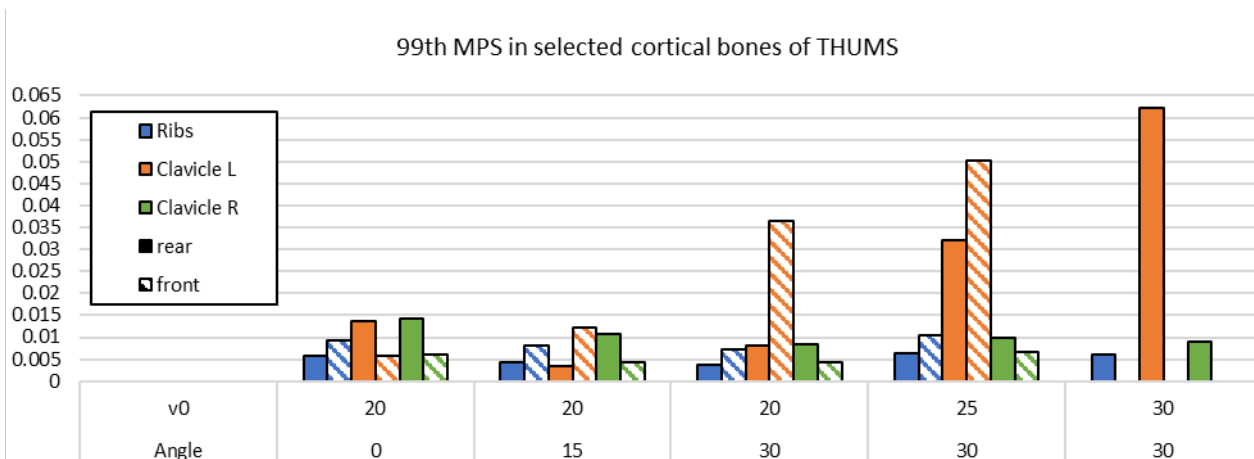*no value could be obtained since an error termination occurred.

Fig. A4. 99th MPS in cortical ribs and clavicles of THUMS sitting in the rear and the front. Solid bars representing the adult sitting in rear, hatched ones representing the adult sitting in the front.
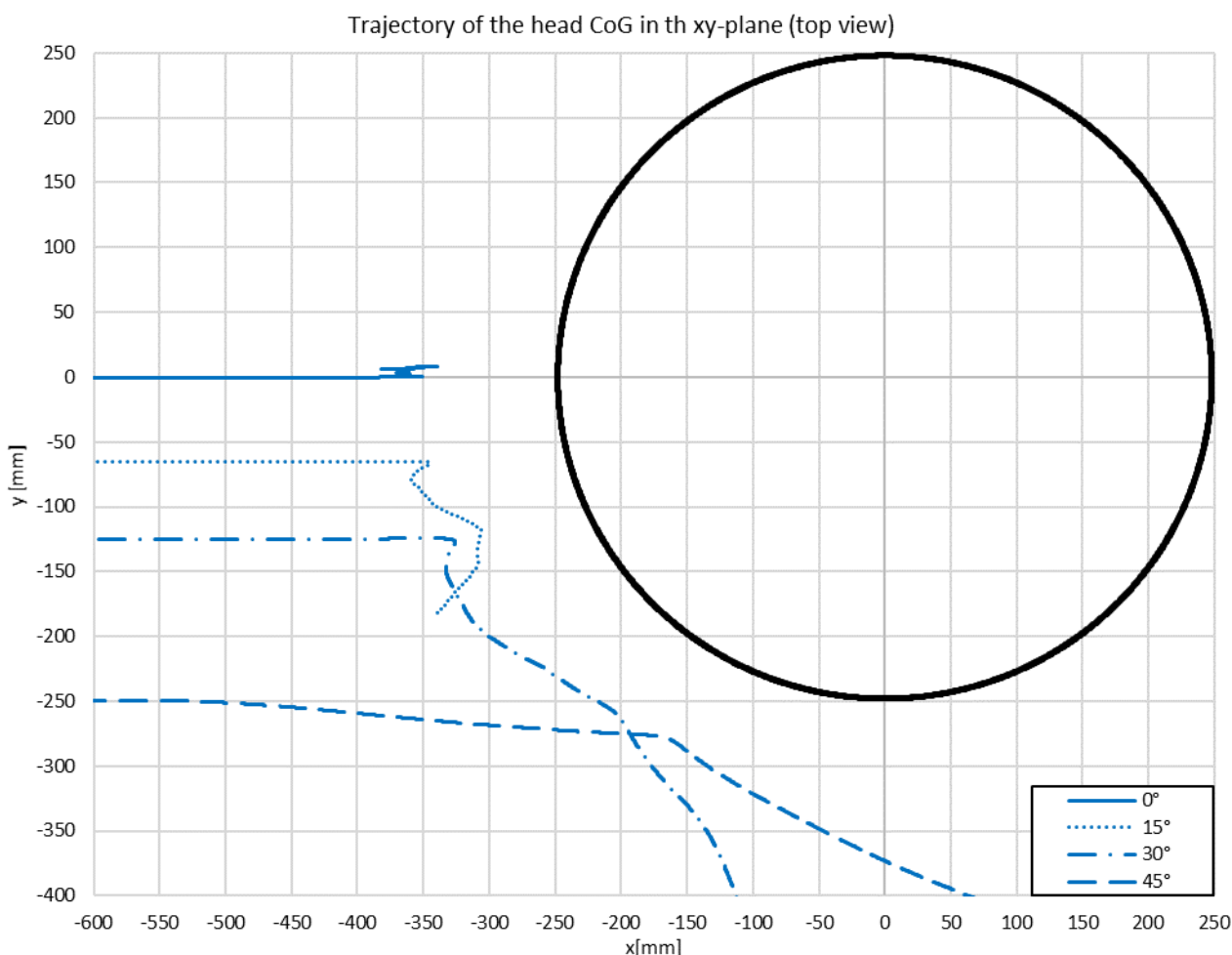

Fig. A5. Head trajectory of the PIPER model (with helmet) impacting the tree at different angles (v_0 = 20 km/h)

Fig. A5 shows the head trajectory of the PIPER model (with helmet) for impacts at 20 km/h and different impact angles. The bold, solid (black) line represents the tree. Offsets were applied to the trajectories, so that the centre of the tree is coincident with the origin of the coordinate system. The sledge rider was approaching the tree starting from the negative x-direction, riding towards positive x.

The solid line shows the trajectory in a frontal impact (0°). After the head impacted the tree it rebounded and some back and forth movement was observed. No lateral movement occurred. The trajectory is quite similar for the 15°-impact (dotted line), although there is a slight sideways motion (y-direction) after the impact. Nevertheless, this does not have a big influence on the injury metrics of the head. In case of a 30°-impact (dash-dotted line) a pronounced sideways movement of the head occurred after the impact. Furthermore, the head

rebound from the tree is not as intense as at 0° and 15°, respectively, explaining the lower head injury values for this case. For the 45°-impact (dashed line), no head rebound occurred at all. Instead the head was only deflected sideways (y-direction), explaining the very low head injury metrics in this impact. The influence of the interaction between sledge and tree on the head kinematics prior to the head impact could only be observed for the 45° impact since there was a slight sideways movement (y-direction) of the head, starting at approximately x = -500 mm). For all other cases, the head was travelling almost without sideways movement until it contacted the tree.
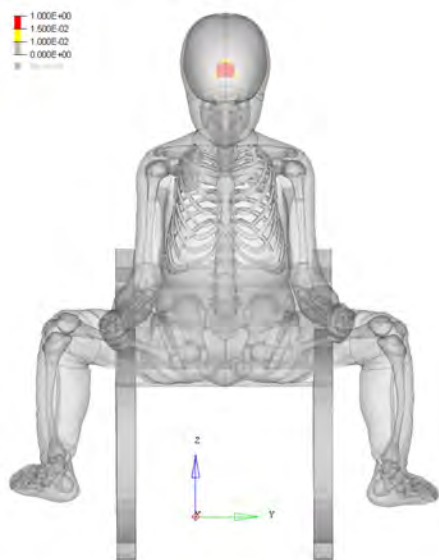
Fig. A6. Head impact of the PIPER model (riding alone, without helmet) in a frontal impact at 20 km/h. Yellow and red areas on the head indicate increased strains.
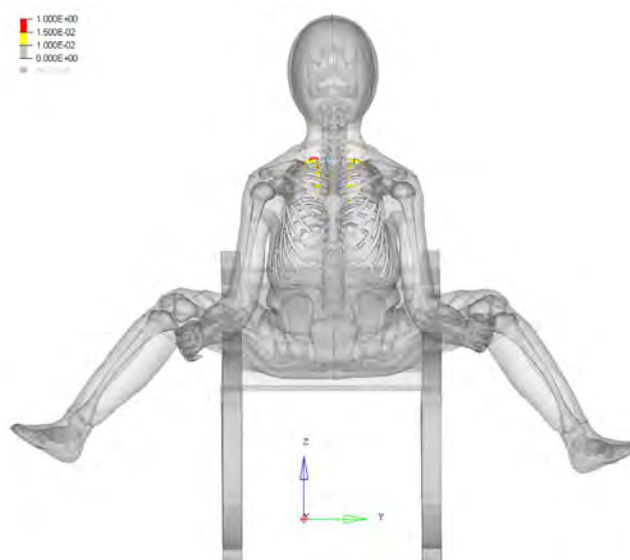
Fig. A7. Rib strains in the PIPER model (riding alone, without helmet) in a frontal impact at 20 km/h. High rib strains (yellow and red areas of the ribs) are induced in the uppermost ribs of the PIPER due to a heavy rebound of the head.
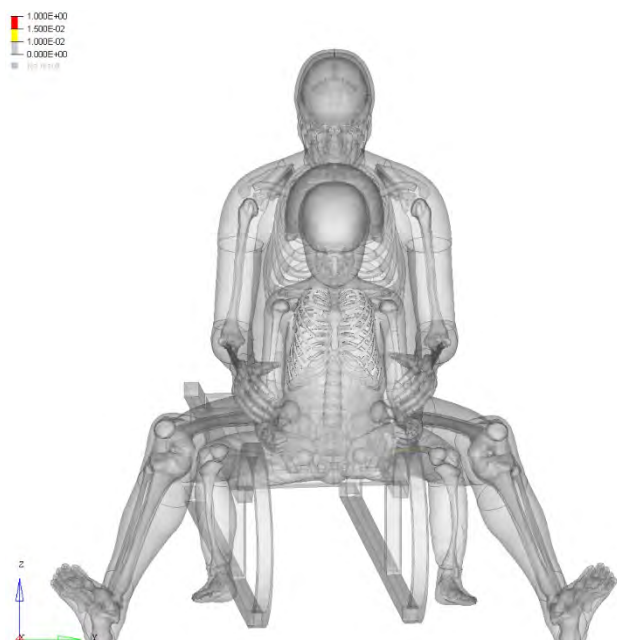
Fig. A8. Force application to the femur of the PIPER due to the interaction with the sledge in an oblique impact (20 km/h; 30°). At this time there is no interaction with the adult person. Yellow and red areas on the femur indicate increased strains.
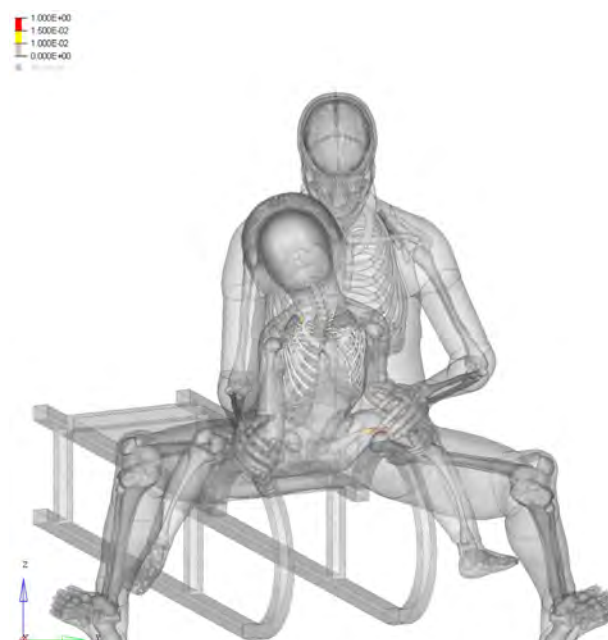

Fig. A9. Strains in the PIPER femur, when being pushed forward by the adult person (oblique impact at 20 km/h and 30°). High strains in the left femur are observed since the adult person is pushing the child into the sled (rigid) and the femur of the child gets stuck between the sledge and the adult person. Yellow and red areas on the femur indicate increased strains.
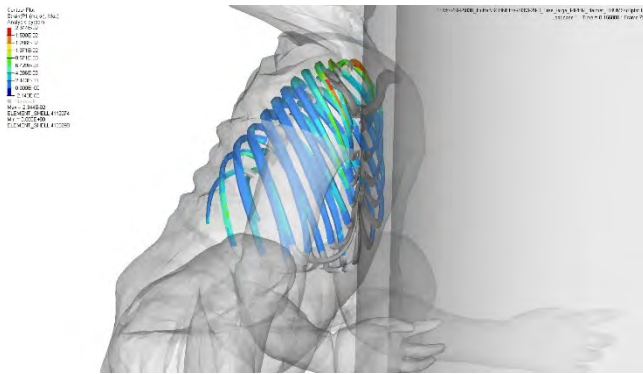
Fig. A10. PIPER rib strains when hitting the tree (child sitting in front of the adult).
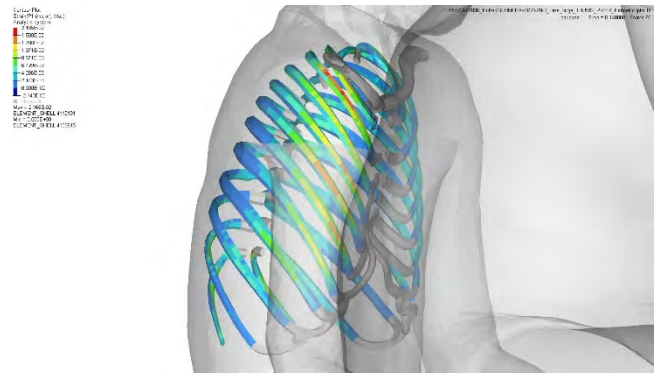

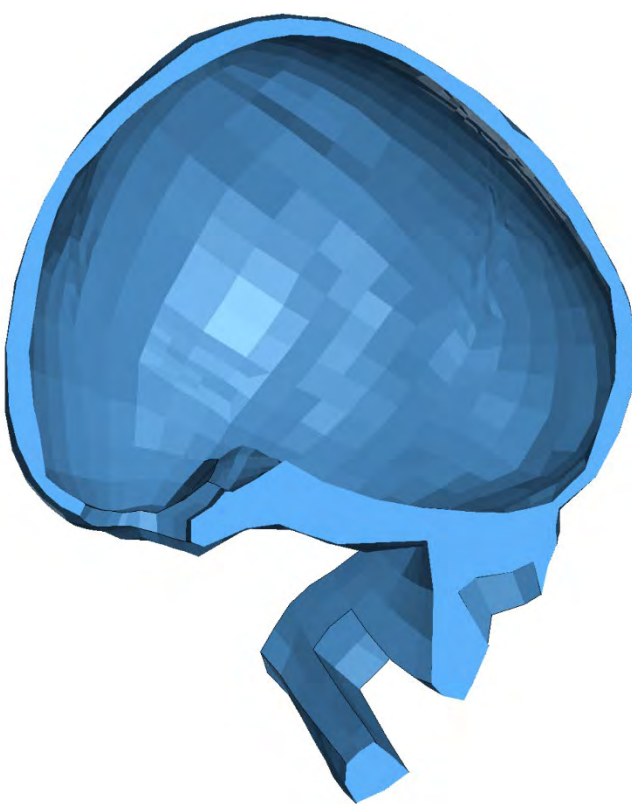Fig. A11. PIPER rib strains when hitting the adult's back (child sitting in behind the adult).

Fig. A12. Section cut of the non-deformed PIPER skull immediately before impacting the tree (frontal impact at 20 km/h).
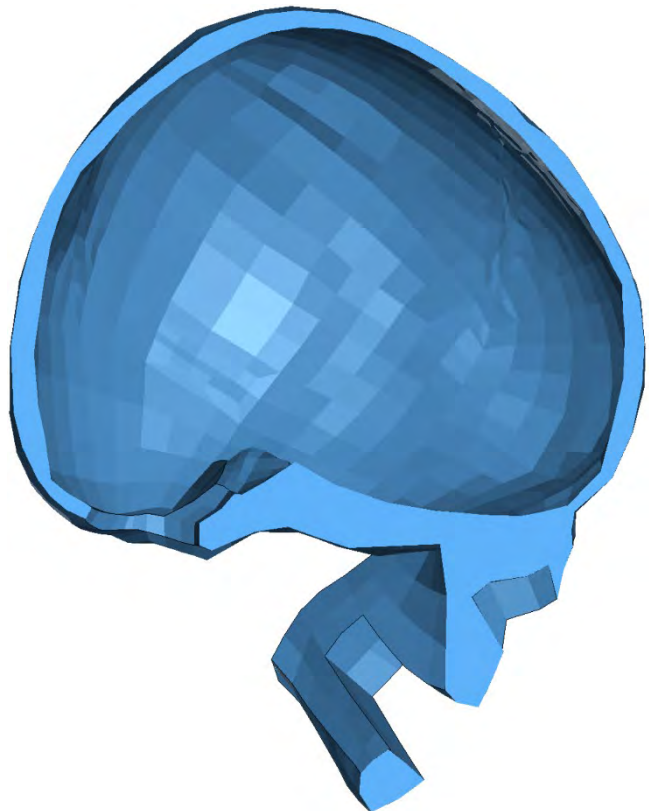

Fig. A13. Section cut of the deformed PIPER skull at maximum deformation (frontal impact at 20 km/h). Only a small amount of deformation was observed.
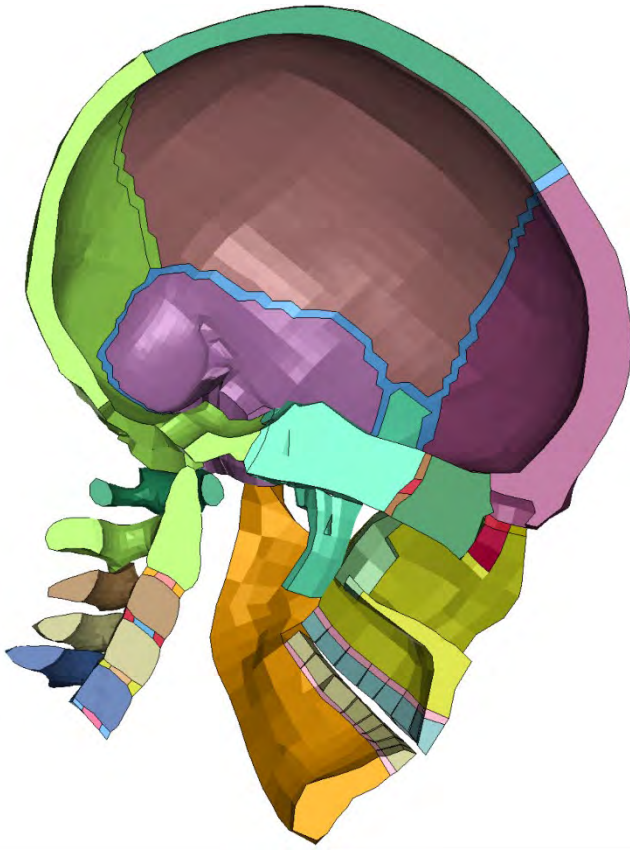
Fig. A14. Section cut of the non-deformed THUMS skull immediately before impacting the tree (frontal impact at 20 km/h; THUMS sitting at the front).
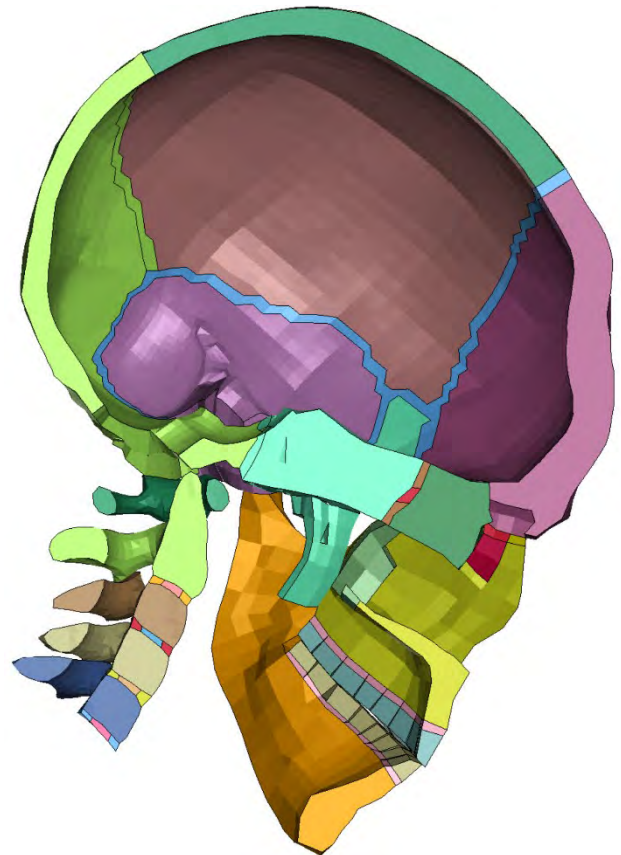
Fig. A15. Section cut of the deformed THUMS skull at maximum deformation (frontal impact at 20 km/h; THUMS sitting at the front). A large amount of deformation was observed.